Proceedings of the 34th International Conference on Ocean, Offshore and Arctic Engineering
OMAE2015
May 31-June 05, 2015, St. John's, NL, Canada

OMAE2015-41808

NUMERICAL INVESTIGATION OF THE INSTALLATION PROCESS AND THE BEARING CAPACITY OF SUCTION BUCKET FOUNDATIONS

Marc Stapelfeldt
IGB Ingenieurgesellschaft mbH
Hamburg, Germany
stapelfeldt@igb-ingenieure.de
(former Overdick GmbH & Co. KG)

Julian Bubel
Institute of Geotechnical Engineering and Construction Management
Hamburg University of Technology
Hamburg, Germany
julian.bubel@tuhh.de

Jürgen Grabe
Institute of Geotechnical Engineering and Construction Management
Hamburg University of Technology
Hamburg, Germany
grabe@tuhh.de

ABSTRACT

This paper was developed in cooperation between the TUHH and Overdick GmbH & Co. KG. The goal of the presented work is gaining further knowledge about the installation and bearing behavior of suction bucket foundations for fixed offshore platforms based on sand.

Buckets are usually made of steel and consist of a cylinder and a lid at the top. They are installed into the sea floor by pumping water out of the buckets to create suction, which drives the bucket into the soil. Suction buckets do not require heavy hammer-equipment for construction like common piles. Thus the installation procedure is much faster and protects the environment significantly by avoiding noise emissions. Therefore, suction buckets are to be considered as a serious foundation alternative compared to steel piles.

For this paper numerical investigations are performed with the finite analyses software ABAQUS. A total of five finite element models – three for the bearing and two for the installation – were created to carry out parametric studies, while using a hypoplastic constitutive model to describe the soil conditions. Therefore, the buckets diameter, embedded depth and the pore-ratio are to be investigated. In addition three different load conditions are applied in the bearing capacity tests: the maximum vertical load, the maximum horizontal load and the minimum vertical load. During the simulation of the installation procedure different pore ratios are tested and it is attempted to simulate an installation by water-extraction.

Based on these numerical investigations it is possible to investigate known and currently more or less unknown phenomena of the bearing and the installation of suction buckets. Thus, a more detailed knowledge about the function of this kind of foundation is to be gained. In addition, the numerical studies are compared to the design-procedure according to API RP-2A-WSD and the DNV CN-30.4.

INTRODUCTION

Suction Buckets used as foundations were first developed in the 1980s at the Gorm oil field at the Danish North Sea. In accordance to reference [1], they were used as anchors for floating structures. Later in the 1980s the concrete-made foundations of the 380 m high Gullfaks C were installed at the Norwegian North Sea. Tjelta, et al. [2] later published an article about the installation of the largest ever build buckets by a combination of self-weight penetration and the application of a suction pressure. In 1995, the well-known Draupner E platform was installed on a steel jacket based on four suction buckets with twelve meters in diameter and six meters of embedded depth. This platform is also located in the Norwegian North Sea and is famous for the well documented hit by a 25.7 m high monster wave back in 1995 [3]. In addition to these pilot projects approximately 500 suction bucket foundations have been installed since the 1990s.

Suction buckets are versatile: It is possible to use them in shallow or deep water and in any kind of soil. Buckets are often used in mooring systems to anchor tension loads from floating deep-water-platforms in clay. In recent years the interest of an application in shallow water depths of less than 50 m has increased. Especially the rapid development of offshore-wind-farms has raised the demand of reducing the cost of platform foundations. This demand has pushed the development of the suction bucket technology in the last few years. Recent research projects were carried out particularly at the Oxford University [4]. The long term goal of these projects and the research done for this paper is to establish suction buckets as a common foundation type for fixed offshore platforms based on sandy soils.

Other than the versatility, the biggest advantage of suction buckets is their short installation time and the lower costs compared to pile-foundations. No heavy hammer is required and

the suction induced penetration takes significantly less time than conventional pile driving. In addition the installation process causes no reasonable noise, so the environment, especially fish and whales, is protected.
As presented, suction buckets have got the potential to replace piles as the standard foundation for offshore platforms, especially in shallow water locations with sandy sea floors like the North Sea. The following investigations provide further understanding of the installation process and the bearing behavior of bucket foundations. In addition the methods and possibilities of the numerical modeling are investigated. Therefore advanced modeling technics are used and presented in the following.

SOIL MECHANIC THEORY

Before the numerical modeling is considered, the soil mechanical processes during bearing, uplifting, and horizontal loading have to be explained. In addition, this section includes an overview about the suction induced installation in sandy soils.

Bearing Mechanisms of Suction Buckets in Sand

The loadbearing in sand differs depending of the load direction, the load velocity and the combination of several loads. In addition each load on a bucket is beard by the unique combination of the skirt that is acting like a pile and the lid, which – if it is in contact with the sea floor – operates like a shallow foundation.
Thus a simple vertical compression load on a fully installed suction bucket is beard by the skin friction of the bucket wall and the compression, which occurs between the buckets lid and the soil below. During fast loading excess pore pressure may occur temporally, depending on the sand's permeability.
During a tensile load the resistance force of a bucket foundation also consists of two parts. First, the skin friction is mobilized at the inner and outer perimeter of the bucket wall. Second: While rapid loading and a sufficiently low permeability of the sand inside the bucket a low pressure occurs due to the vertical movement. The increasing gap between the mud line and the lid is to be filled with pore water, but the flow velocity of the required seepage is too slow to fill this void immediately. As the result low pore water pressure occurs temporally, which increases the uplifting capacity. This mechanism is also called "reverse bearing". Tjelta, et al. [3] confirmed the occurrence of the low pressure inside of buckets installed in dense sand, loaded with a single tensile load.
At offshore platforms the cyclic change of loads due to wind and waves should also be considered. During a storm a bucket foundation may have to bear tensile loads more than once, especially when a light topside, like an offshore wind energy plant, is installed. Even recent research by Kelly, et al. [5] and Houlsby, et al. [6] does not clarify if a suction bucket foundation is able to bear cyclic tensile loads. It was found that buckets under pure cyclic compression loads fail due to bearing failure. However if the load direction changes cyclically or cyclic uplifting loads are applied on buckets, a pullout failure will occur. If the low pore water pressure is also increasing the reverse bearing capacity during cyclic loading is still to be explored. Further research is highly recommended, because it could clarify whether it is possible to design suction buckets for tensile loads in sand.
In addition to the vertical loading the horizontal load bearing of suction-bucket-founded jackets due to wave and wind loads is also taken into account here. Like the vertical bearing, the horizontal bearing also works by two mechanisms. First, the passive lateral earth pressure at the front side of the skirt resists the lateral movement induced by lateral loading. At the back of the bucket the soil is loosened and the active lateral earth pressure increases the horizontal load. Second, there is a shear force occurring at the area below the bucket. The soil that is surrounded by the skirt is moved with the bucket during horizontal loading. Thus, soil internal friction occurs at the level below the bucket wall's tip. This shear resistance depends on the corresponding vertical load. Therefore, a heavy vertical load increases the shear resistance.

Installation Procedure of Suction Buckets in Sand

The installation procedure of suction buckets in sand differs from the procedure in clay, like Houlsby & Byrne [7] describe in their paper. Nevertheless, the procedure is also separated into two steps: the self-weight-penetration and the suction pressure installation.
During the suction installation in sand, a special mechanism occurs. The extraction of water causes a seepage flow from the mud line outside of the bucket, down the outside of the wall, around the tip and up to the pump at the bucket lid. This seepage flow increases the friction at the outside of the skirt and decreases it at the tip and at the inside of the skirt. Due to this mechanism, the bucket penetrates into the soil, while applying only low suction pressure.
These low pressure installation is necessary, because the pressure is limited by the pressure that causes piping failure in addition to the cavitation limit. If piping occurs, the sand particles at the seepage path will be washed out and the effective stresses will reduce gradually. Piping failure actually occurs, when the effective stresses become zero locally. At these certain spots pipes occur. Water is able to flow into the bucket through these pipes and the suction pressure decreases, what causes a refusal and the installation fails.
The piping limit depends on the length of the seepage path and the specific weight of the soil. Therefore, the depth of the self-weight-penetration is crucial. The bucket has to be penetrated deep enough into the soil, so that suction pressure can be applied without piping failure. Thus, the installed structure has to be heavy enough or flooded partially to increase its weight.

NUMERICAL MODELLING

The five numerical models that were used to perform the analyses are made with the finite element analyses (FEA) software ABAQUS. During the modelling process the implicit and explicit solver and the Coupled Eulerian Lagrangeian (CEL)

Method was used. In addition, the zipper technic, presented by Henke [8], was utilized and improved. In some models it is required to simulate the pore pressure, so the according modeling technic was chosen under this consideration. The following sections give an overview of each of the five models.
Each model was checked in terms of geometry, initial and boundary conditions and mesh configurations as well. The soil model was checked by recalculating oedometer and triaxial laboratory tests.

Soil Properties

For the calculations a hypoplastic constitutive soil model including inter granular strains, introduced by von Wolfersdorf [9] and Numunis & Herle [10], of the "Cuxhavener Sand" (CSH) was used. Dense, medium dense and lose soils were investigated by varying the void ratio from 0.8 to 1.1. The friction angle φ' was varied from 34 ° to 40 ° and the stiffness modulus E_S was varied from 29 MN/m² to 58 MN/m². The dilatancy angle is 0.4 °. For the hypoplastic model the following parameters from Table 1 were used:

TABLE 1: HYPOPLASTIC SOIL PARAMETERS

Parameter	Value	Unity
φ_C	0,576	[°]
n	0,116	[-]
h_S	4767000	[MPa]
e_{d0}	0,60	[-]
e_{c0}	1,22	[-]
e_{i0}	1,403	[-]
α	0,147	[-]
β	1,36	[-]
R	9,458e-04	[-]
m_R	2,0	[-]
m_T	6,304	[-]
X	1,485	[-]
β_r	0,936	[-]

Bucket Geometries

The investigated suction buckets have diameters D between 3 m and 12 m and embedded depth L of 3 m to 9 m. Therefore buckets with L/D ratios between 0.25 and 1 are simulated in two- and three-dimensional analyses.

Vertical Bearing Capacity Model

Calculating the maximum vertical bearing capacity of a suction bucket requires a FE model that resists significant mesh deformations. For slow loading and no excess pore pressure is expected, a coupled soil- pore water simulation is not necessary. In this case an radially symmetric implicit model type is chosen. The applied load is solely in vertical direction
The mesh around the skirt tip needs detailed attention since this area exhibits the largest deformations and the elements are small and slim here. To avoid calculation instabilities due to mesh destruction, the zipper technic was used in a special way. Normally a small gap filled with a rigid body is placed below the tip of the penetrating member (bucket). This tube does not interact with the penetrated member, so during the downward movement of the bucket, the skirt moves through the tube and the surrounding soil makes contact with the skirt, while simultaneously losing contact from the tube. Whereas the shaft friction is fully applied, the tip resistance of the skirt is underestimated with this technic. Due to further numeric instabilities it was required, that the tube width equals the skirt's wall thickness.
Therefore the tip resistance is neglected in this model, but the resulting mistake is not noticeable, because the resistance at the skirt's tip contributes is irrelevant compared to the residual force at the bucket's lid. Thus, it is possible to calculate the maximum bearing capacity and settlements adequately with this model.

Cyclic Pullout Capacity Model

During the calculations for the pullout, the cyclic pullout and the respective bearing capacity no excessive settlements are expected. However, significant positive and negative pore pressures are about to occur due to rapid loading. Thus a model that includes pore water soil coupling is required but the application of the zipper technic is not necessary. No load inclination or horizontal load will be applied, so it is possible to use a radially symmetric model again.
The corresponding analysis is split into two parts. First, the maximum uplifting capacity is calculated with and without the influence of the pore water (partly drained and drained) by single load controlled analysis. Second, cyclic loads are applied in four steps. Therefore, four load steps with 20 cycles each and a loading period of ten seconds per cycle are introduced. The pressure load amplitudes amount to 5 kN/m² for step 1, 10 kN/m² for step 2, 20 kN/m² for step 3 and 40 kN/m² for step 4. By increasing the load step by step, the maximum capacity for cyclic compression loads, cyclic tension loads and cyclic altering loads, which switch between compression and tension, are calculated.

Horizontal Bearing Capacity Model

The horizontal bearing is a three-dimensional problem, therefore a three-dimensional model is required. Fast loading rates are not expected, so the pore water soil coupling is not necessary. Only small settlements are expected to occur.
According to these requirements a half-circle three-dimensional model without pore pressure degree of freedom is designed. With this model horizontal capacities are calculated. In addition it is possible to apply different vertical loads. The analyses were performed with no vertical load, a 1,000 kN compressional load and a 1,000 kN tensional load. The horizontal load tests are performed by distance controlling via boundary condition.

CEL Installation Model

The Coupled Eulerian-Lagrangeian (CEL)-Method is an explicit, three-dimensional analysis type. The CEL model

consists of an eulerian area (soil) and a lagrangeian area (bucket). The lagrangeian bucket is penetrated into the eulerian soil. Due to the properties of an eulerian mesh, the nodes do not move, but the mass inside the elements moves. Thues the penetration of the bucket's skirt does not destroy the mesh. The only weakness of this method is, that a pore pressure simulation is not yet possible in ABAQUS.
Nevertheless a CEL model is used to calculate the jacket installation of a bucket. Therefore, the eighth of a soil cylinder is modelled as an eulerian area and an eighth of a suction bucket is the lagrangeian part. The bucket is pushed in the desired depth and thus the pore water flow during suction is not included in the results.

Explicit Installation Model

The ABAQUS explicit installation model is the most advanced model used in this work. It is a two-dimensional model including the zipper technic and a pore pressure soil coupling. This is done by an implemented user subroutine (VUMAT), which incorporates the hypoplastic constitutive model according to von Wolfersdorf [9] with the extension of inter granular strain according to Nimunis & Herke [10] for the soil skeleton coupled with the pore water pressure. The subroutine also allows the pore water pressure transfer through openings and cracks, which is crucial for the zipper technic tube to not artificially separate the soil in two not corresponding parts [11]. This model allows a realistic simulation of the suction pressure installation. The suction pressure is applied by simultaneous loading of the bucket and a decrease of the hydrostatic pressure at the mud line inside the bucket, both of the same magnitude.
As mentioned, this type of model includes a lot of advanced modelling technics. It uses a new variation of the zipper technic and special boundary conditions. However the model has a significant weakness: The calculation of a few millimeters of penetration takes days – even with a high-power compute-cluster. So there will be no results presented. Nevertheless, this new modeling approach shall be presented and it may be possible to calculate this model with more powerful processors in the near future.

RESULTS OF THE BEARING ANALYSES

In this section the results of the numerical analyses are presented. The total of the load scenarios and the simulation of the installation procedure are provided in the following sub sections.

Vertical Bearing Capacity

In this sub section the bearing capacity studies are presented. First the stresses and deformations caused by vertical loading are analyzed. Therefore Figure 1 presents the vertical stresses of a suction bucket embedded in sand. It is shown that there are increasing stresses inside and below the bucket. The outer stresses close to the skirt are only slightly increased. The maximum stresses occur inside the bucket near the skit tip and follow a reverse cone from underneath the bucket, see Figure 1

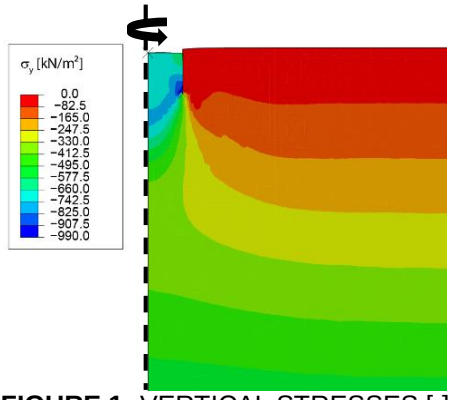

FIGURE 1: VERTICAL STRESSES [-]

The consideration of the displacements, presented in Figure 2, shows that the soil inside the bucket moves downwards. The soil close to the outside of the skirt also moves downwards. The soil below the bucket moves downwards and to the right. Shear failure planes are not visible. In addition it has to be noticed that the deformation of the soil decrease with an increasing distance from the lid. Thus, the soil inside the bucket is compressed and therewith the void ratio decreases.

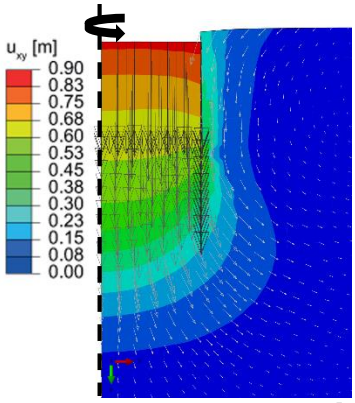

FIGURE 2: DISPLACEMENT [M]

From these graphical results of the bearing mechanism of suction buckets stress-displacement-curves were derived. These curves show no bearing failure, even with vertical settlements of nearly 90 cm. They follow a typical development, which is presented in Figure 3. The curves in Figure 3 also show the total vertical load (RF_y) is splitted up into two shares: the skin friction (CF_y) and the contact force between the lid and the soil (PF_y). As presented, the skin friction bears approximately 20 % of the total load, the residual transmitted by contact pressure at the lid.

Figure 3 also presents curves for different buckets. The first two numbers in the legend indicate the embedded depth L and the last two indicate the diameter D, for example 0612 is a bucket with L = 6 m and D = 12 m. The used diameters in Figure 3 are always 12 m, thus only the embedded depth changes. That variation causes not only an incensement of the skin fiction, it also seems to increase the pressured force at the lid at the same stage of displacement.

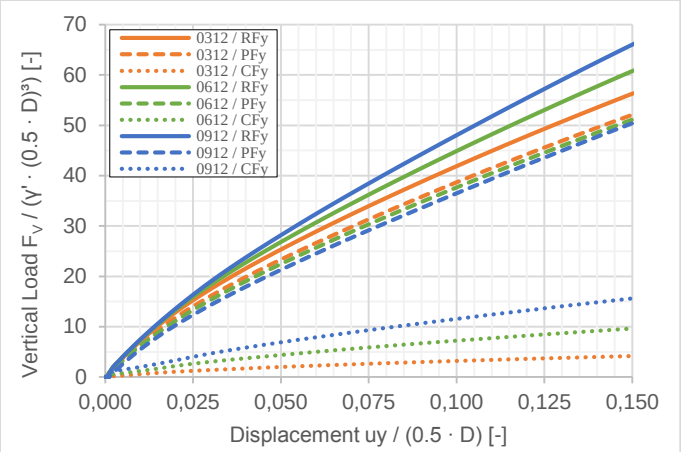

FIGURE 3: LOAD-DISPLACEMENT-CURVES

A further investigation considering different bucket diameters, settlements and void ratios leads to the relationship between these parameters and the respective vertical load presented in the following Figure 4.

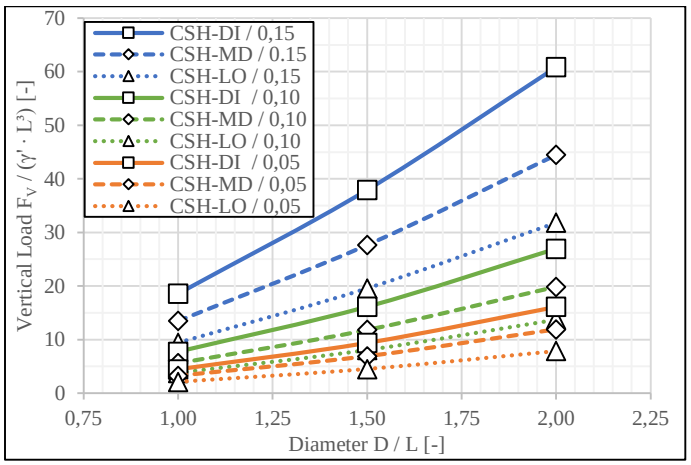

FIGURE 4: VERT. LOAD F_V VS. DIAMETER D

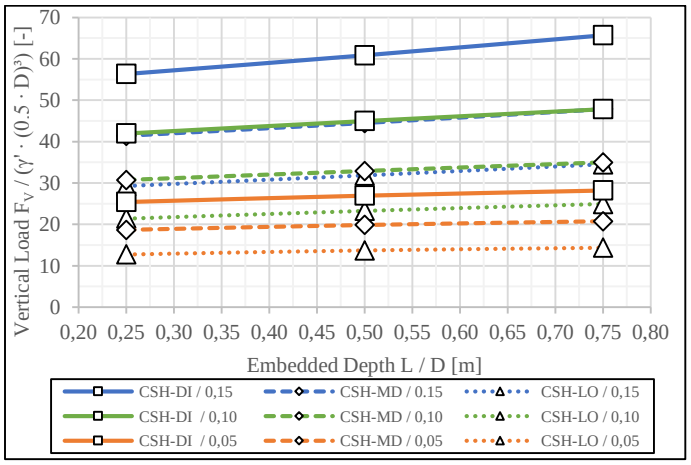

FIGURE 5: VERT. LOAD F_V VS. EMBEDDED DEPTH L

Figure 4 presents buckets embedded in dense (DI), medium dense (MD) and loose (LO) Cuxhavener sand. The presented curves show the influence of the settlement (0.05·L; 0.10·L; 0.15·L) and the diameter as D/L ratio (1; 1.5; 2). The influence of the embedded depth as L/D ratio, is presented in Figure 5.

A comparison reveals, that a larger diameter increases the bearing load in sand more than a deeper embedment. This matches the observation from Figure 3. The load bearing share of the skin friction is small and the secondary effect of the deeper embedment of shallow foundations is of minor relevance.

An additional investigation of the spatial distribution of the vertical and horizontal strains shows, that there is a considerable compression inside and below the bucket and some loosening up close to the outer skirts wall, visible in Figure 6.

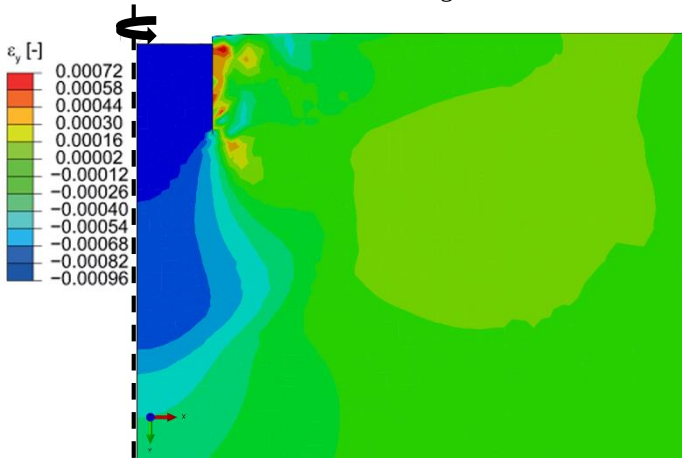

FIGURE 6: VERTICAL STRAIN [-]

In addition, horizontal strains, occur outside the bucket. Figure 7 presents these horizontal strains, showing compression due to the horizontal displacement of soil underneath the bucket and loosening of soil due to slight lifting likewise because of the displacement.

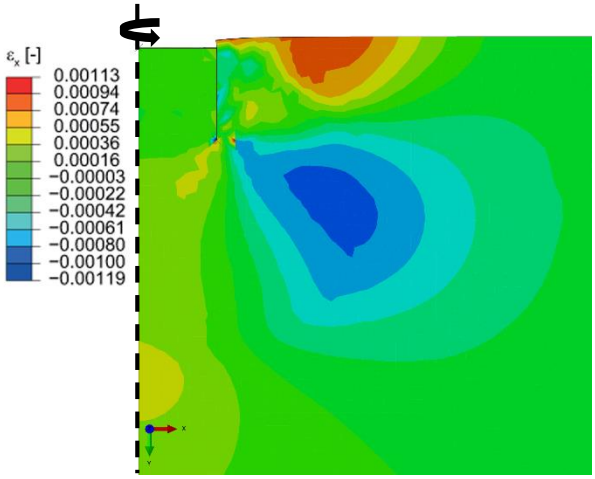

FIGURE 7: HORIZONTAL STRAIN [-]

The stress and strain relationship presented in this sub section demonstrates two effects that are typical for the bearing behavior of bucket foundations: Buckets are able to bear heavy loads including the occurrence of large settlements without failure. Simulated buckets with 90 cm of settlement did not fail due to bearing. But during the load bearing, the void ratio inside

the bucket decreased gradually. This so called cushion effect inside the bucket enables the bearing of heavy loads including large deformations without failure. These observations match with the results presented by Villalobos referred in [9].

Pullout Capacity

The pullout capacity of suction buckets is mainly influenced by the soil's drainage situation and the loading velocity. During rapid tensile loading pore water underpressures occur inside the bucket. This underpressure increases the tensile capacity in comparison to a bucket which is loaded slowly. The curves in Figure 8 present the results of rapid and slowly loaded buckets.

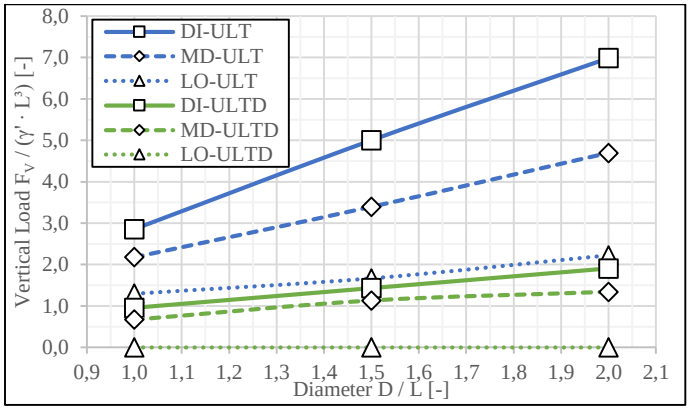

FIGURE 8: VERT. LOAD VS. DIAMETER D

The sand around the bucket reacts drained during slow loading (ULTD) and partly drained during rapid loading (ULT). In addition, the ultimate pullout capacities are presented depending on the bucket diameter. The ultimate pullout capacities depending on the embedded depth are presented in Figure 9.

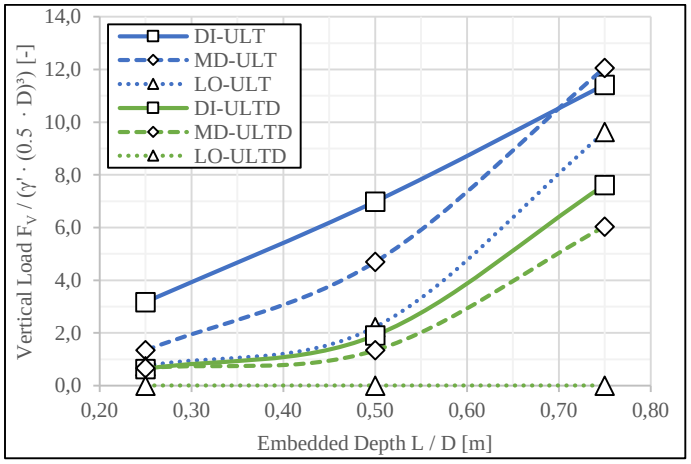

FIGURE 9: VERT. LOAD VS. EMBEDDED DEPTH L

The presented relations show that the ultimate tensile capacity in partly drained conditions is much higher than in fully drained conditions. Furthermore, the void ratio influences the tensile capacity, as presented in Figure 10.

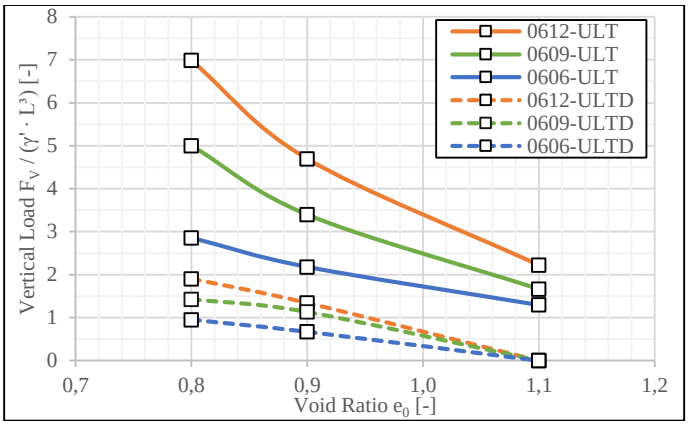

FIGURE 10: VERT. LOAD VS. VOID RATIO & D

The curves show that the capacity decreases with an increasing void ratio. In loose sand (e = 1.1) there is no tensile capacity. Both, bucket diameter and skirt length influence the tensile capacity. The effect increases for fast loading with partly drained conditions. The skirt length is of higher importance than the diameter as presented in **Figure 10** and **Figure 11**. The skirts wall friction drives the tensile capacity and thus larger skirts and higher bulk densities distinctly increase the capacity, also considerably for drained conditions.
However it is shown that the loading velocity influences the drainage situation and due to the drainage the ultimate tensile capacity increases or decreases. These results match the findings of Houlsby, et al. referred in [6].

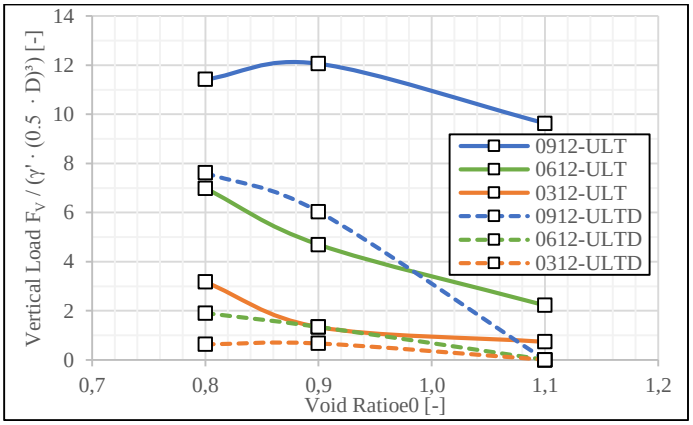

FIGURE 11: VERT. LOAD VS. VOID RATIO & L

Cyclic Pullout Capacity

In addition to the single tensile loads cyclic loads are investigated. During cyclic vertical loading the load direction is crucial. Therefore numerical calculations including compressional, tensional and alternating loading are performed. Typical results are presented in Figure 12 and Figure 13.

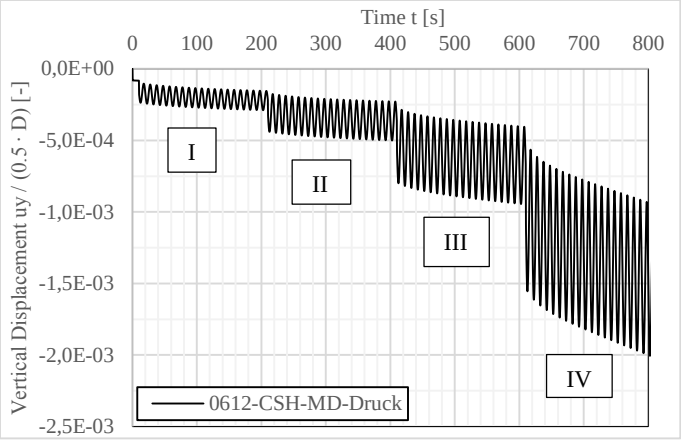

FIGURE 12: TIME VS. DISPLACEMENT

Figure 12 shows that the displacements in load step one and two are almost elastic. In load step three and even more in load step four plastic deformations occur and the total displacements increase gradually. The force displacement plot in Figure 13 presents a similar observation. Thus, a hysteretic development of the load displacement curve occurs.

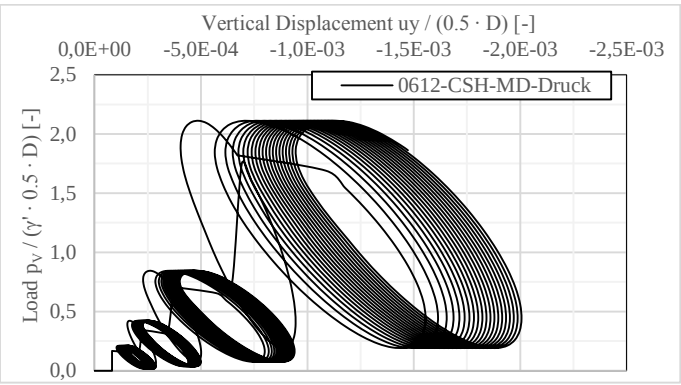

FIGURE 13: LOAD VS. DISPLACEMENT

Because the loads were applied rapidly in periods of 10 s the drainage and the effective stresses are to be considered. Figure 14 presents the effective stresses under cyclic compressional loading, normalized by the initial stresses.

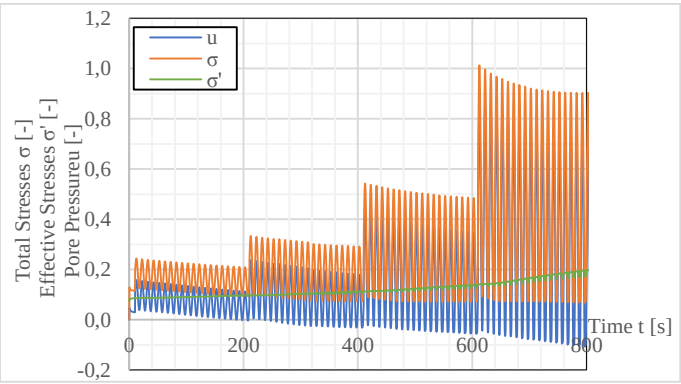

FIGURE 14: EFFECTIVE STRESSES (COMPRESSION)

The pore pressure bears a notable part of the total load. But the share is reduced during the test. Thus, residual pore pressures are degraded gradually while the effective stresses increase.

The consideration of the test with alterning tensile and compressional cyclic loads reveal that the soil bucket interaction is different. Figure 15 shows that the stresses and pore pressures are almost constant during the first three load steps. In load step four the stresses and pore pressures increase dramatically and after a few cycles the bucket is pulled out of the soil.

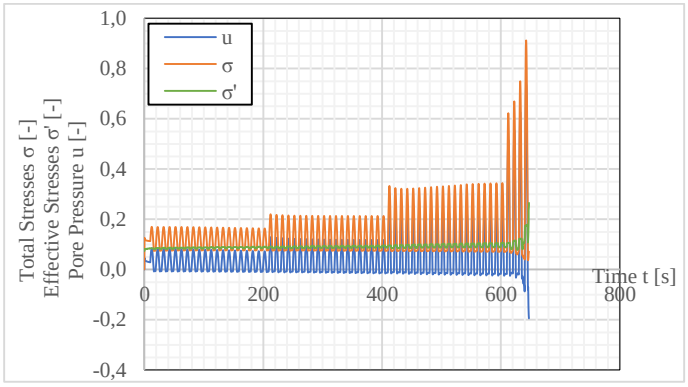

FIGURE 15: EFFECTIVE STRESSES (ALTERNING LOAD)

The effective stresses and the pore pressures occurring during tensional loading show an analog behavior. The development of the curves during each load step differs with a significant decreased pore pressure in step 3, but the pull out after increasing the tensional load in step 4 is similar.

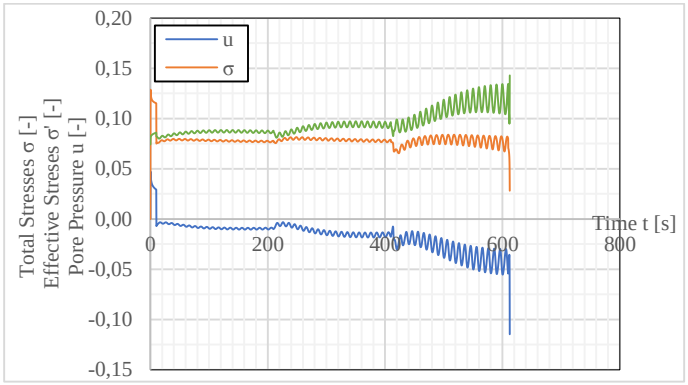

FIGURE 16: EFFECTIVE STRESSES (TENSION)

These results show that there is a different response depending on the load direction. During cyclic compressional loading no failure occurs. During cyclic alterning or tensional loading a pull out failure occurs shortly after the transition to the fourth load step.

Horizontal Bearing Capacity

The capacity against horizontal loading consists of two parts: The passive earth pressure at the skirt and the shear force at the bottom level below the skirt. Both effects are shown by numerical simulations, as Figure 17 presents.

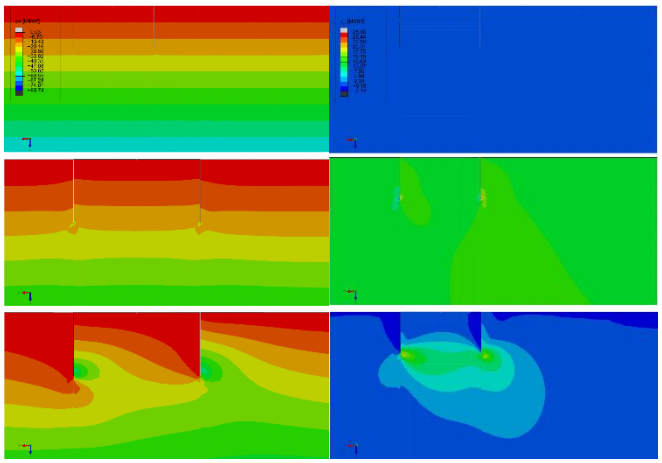

FIGURE 17: EMBEDMENT AND SHEAR RESISTANCE

The influence of the void ratio and the vertical load in addition to the horizontal load was investigated and the results are presented in Figure 18. As presented, both parameters influence the horizontal bearing behavior.

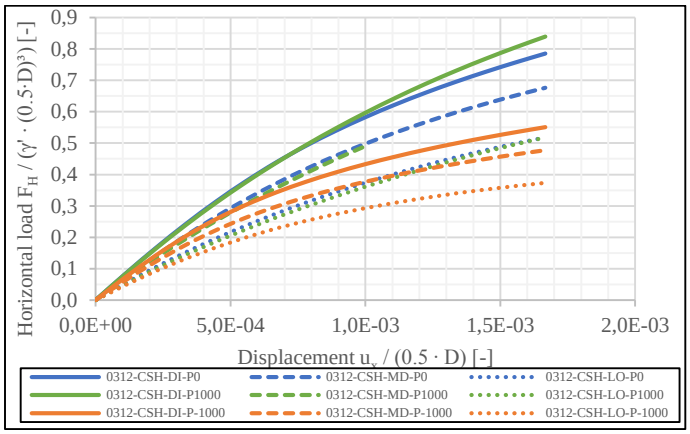

FIGURE 18: LOAD VS. DISPLACEMENT

Increasing the vertical load, results in a higher horizontal capacity. However, there is almost no difference between the results for P = 0 kN and P = 1,000 kN.In addition it is shown that the capacity in dense sands with small void ratios is considerably higher than the capacity in loose sand with high void ratios.

RESULTS OF THE INSTALLATION ANALYSES

Due to the issues concerning the usage of ABAQUS EXPLICIT to simulate the installation procedure, only the results of the CEL-Model are presented here. The results of this jacking installation are presented in the following sub section.

CEL Installation Model

The results of the installation in loose, medium dense and dense sand are presented in Figure 19. Each curve represents the resistance against the penetration of the skirt. All three curves increase to a specific maximum. After a penetration of approximately 50 % of the total skirt length the maximum resistance is reached.

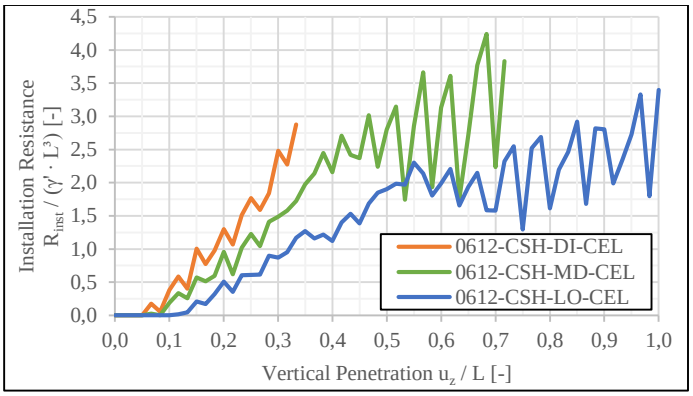

FIGURE 19: INSTALLATION RESISTANCE

It is to be noted, that no refusal occurs. The abrupt end of the orange and green curve is due to an expiring runtime of the calculation. Nevertheless, the presented curves are considered to be sufficient to estimate the installation resistance of the investigated bucket.

Furthermore it has to be noted, that the jacked installation neglects the effects of the seepage flow. Instead of the loosening effect next to the skirt and especially below the tip, a compression of the soil occurs in these locations. Due to these circumstances, the installation resistance is overestimated.

COMPARISON WITH LITERATURE DATA

A comparison with data from literature is hardly possible, because the soil conditions and loading scenarios are normally unequal. In this case a comparison of the cyclic vertical loading test with the data measured at the Draupner E and reported by Tjelta in reference [3] is possible and presented in Table 2.
The buckets of the Draupner E and the tested buckets have the same diameter, embedded depth and wall thickness. And both buckets are installed in sandy soils. Thus a comparison of both results is reasonable.

TABLE 2: COMPARISON WITH DRAUPNER E DATA

Parameter		Draupner E		0612-CSH-DI-Compr.	0612-CSH-DI-Change	0612-CSH-DI-Tensile
		C1-Bucket	A3-Bucket			
Diameter	D [m]	12.0		12.0	12.0	12.0
Embedded Depth	L [-]	6.0		6.0	6.0	6.0
Period	T [s]	11.2		10.0	10.0	10.0
Wall Thickness	t [mm]	40.0		40.0	40.0	40.0
Density	I_n [%]	90.0		67.8	67.8	67.8
Vertical Load	$F_{V,max}$ [kN]	-	17500	10549.6	8097.1	1334.1
	$F_{V,min}$ [kN]	-14500	-	-	-4872.3	-14008.6
	$F_{V,max}$ [-]	-	8835	5326	4088	6074
	$F_{V,min}$ [-]	-7321	-	0.000	-2460	-7072
Displacement in z-Direction	$u_{z,max}$ [mm]	4.190	3.650	0.000	4.354	0.911
	$u_{z,min}$ [mm]	-3.270	-4.610	-0.842	-1.000	-0.031
	$u_{z,max}$ [-]	0.007	0.006	0.000	0.007	0.002
	$u_{z,min}$ [-]	-0.005	-0.008	-0.001	-0.002	0.000

The comparison shows similar maximum and minimum loads for the numerical analyses and the storm described in Tjelta's report referred in [3]. Thus, this comparison is considered as an additional confirmation to the performed numerical studies. Since different soil properties apply the displacements reported and calculated differ insignificantly.

COMPARISON WITH THE API AND DNV RULES

A comparison between the numerical investigations and analytical calculations was performed for each calculation. The formulas according to API RP-2A-WSD [10] and DNV CN-30.4 [11] are used. The results are summarized below:
The comparison of the vertical bearing analyses reveal the following observations:

- The analytical capacities are utilized up to 72 % by the numerically calculated loads.
- The utilizations are higher while using the formula according to API-rules.

The comparison of the vertical tensile loading analyses reveal the following observations:

- The analytical capacities are utilized up to 437 % by the numerically calculated loads.
- The occurrence of a low pore water pressure is not considered by the analytical equations, thus the analytically calculated capacity could dramatically underestimate the actual capacities.

The comparison of the horizontal bearing analyses reveal the following observations:

- The analytical capacities are utilized up to 474 % by the numerically calculated loads.
- The unity checks including zero or tensional vertical loading are impossible to perform.

The comparison of the installation resistance analyses reveal the following observations:

- The numerical results are similar to the analytical results.
- Except the highest expected value of the calculations in accordance to the DNV rules: This value exceeds the limiting piping pressure.
- No other resistance value exceeds the piping nor the cavitation limit.
- Each performed analytical calculation and FE simulation neglect the seepage flow and its resistance decreasing effects.

CONCLUSIONS

In the following paragraphs the results of the numerical analyses are summarized and discussed as well as conclusions are found. First, the results of the vertical bearing analyses are to be reviewed:

- Buckets bear vertical loads by the skin friction force (approx. 20 %) and a pressure force at the lid (approx. 80 %). Thus buckets should be considered as a kind of shallow foundation (depending on the L/D ratio).
- Deeply embedded skirts are unnecessary for heavy load bearing, beside for strong tensional loads.
- Settlements of 90 cm occurred without failure.
- A cushion effect was shown, which means that it is possible to bear large deformations by compression of the sand inside the bucket.
- Heavy loads could be beard even in loose sand, if the related platform's structure is able to resist large settlements.
- The analytical equations do not consider settlements but allow quite heavy loading. Thus an additional settlement calculation is to be performed during the design process.

Based on this findings, suction buckets with short skirts and large diameters shall be designed for the utilization in sand. These buckets are able to bear heavy compressional loads, but the settlements are to be investigated carefully.

Next, the tensile vertical loading is going to be discussed:

- Deeply embedded skirts increase the tensile capacity by increasing the wall friction in analogy to piles
- The loading velocity and the resulting drainage situation are crucial for the tensile load bearing.
- Due to rapid loading nearly undrained or partly drained conditions occur in sand.
- Under slow loading normal drained behavior occurs.
- During partly drained conditions a tensile capacity is provide by low pore water pressure inside the bucket.
- The strength of the low pore pressure is related to the void ratio and the permeability of the sand.
- During cyclic loading, the load direction is crucial. A failure due to compressional loading never occurred. A pull out failure due to tensile or changing load directions occurred frequently.
- It is to be noted, that the pull out failure occurred suddenly after the load increased. Furthermore this kind of failure leads to an overturning of the related platform.
- It is found that small cyclic tensile loads could be beard by suction buckets. But these findings have to be handled carefully because of the extraordinary danger due to overturning failure.
- Analytical methods provide conservative but inaccurate results because of neglecting the low pore water pressure.

Summarizing it was found, that a low pore water pressure occurs due to a tensional loading direction. Thus, it is possible to bear loads that exceed the skin friction. In addition it is possible to bear small cyclic tensional loads by mobilizing this mechanism.

Now the horizontal bearing capacity is reconsidered:

- Horizontal loads are beard by the passive earth pressure at the front side and the shear force at the embedment level below the skirt's tip.
- The combined vertical loading influences the capacities. Thus, a large vertical load increases the horizontal capacity.

- It is considered to be possible, that the cushion effect reduces the shear friction at the bottom of the bucket.
- Analytical methods deliver conservative but inaccurate results. Horizontal loads could not be beard without the presence of compressional loads. Thus, these equations are considered to be inappropriate for sliding checks for slightly vertical loaded platforms.

It is to be noted, that horizontal loads could be beard even without heavy vertical loading, but the capacity increase due to the vertical load is strong. Thus it is recommended to design fixed suction bucket platform as heavy as possible, if uplifting forces due to moment loading occur.
The last investigation to be discussed is the simulation of the installation procedure:

- A CEL calculation could only be performed excluding the pore water simulation. Thus a jacked installation is calculated.
- During this type of installation in sand, the soil is compressed gradually below the skirt's tip. Therefore, the installation resistance increases to a level that is not plausible.
- The analytical procedures according to API and DNV rules have the same weakness. Thus, the predicted resistances against installation in sand are heavily overestimated. Sometimes even the piping limit is exceeded.
- Therefore both methods, numerical and analytical, provide conservative but inaccurate results because of neglecting the seepage flow and its resistance decreasing effect.

As a concluding remark it is noted, that the available methods, including the newly introduced CEL simulation, are not able to calculate the installation resistance accurately. Therefore, a large potential of further research exists.

As a result of reviewing the presented calculations, some further numerical research projects could be developed. With the help of sophisticated FE software and appropriate constitutive models for the soil it is possible to perform adequate vertical bearing analyses with compressional, tensional and even cyclic changing loads. If a second load direction (e. g .a horizontal load) is introduced, a three dimensional analysis is required. With this certain analyses it is nearly impossible to simulate noticeable deformations with material bonded mesh methods. The meshing of the small skirt tip is challenging the numerical stability of the model. Thus mesh free methods or methods like ABAQUS CEL seem to be the next step, but it is still to be proven if today's processor performance is sufficient for computing that kind of models.

ACKNOWLEDGMENTS

I am thankful for my stay at Overdick GmbH & Co. KG and the great support I experienced there. I also would like to thank the Technical University Hamburg-Harburg for the assistance.

REFERENCES

[1] D. Senpere und G. A. Auvergne, „Suction Piles - A Proven Alternative to Driving or Drilling," in *OTC 4206*, Houston, 1982.

[2] T. Tjelta, P. M. Aas, J. Hermstad und E. Andenaes, „The Skirt Piled Gullfaks C Platform Installation," in *Proceedings of the Offshore Technology Conference*, Houston, 1990.

[3] T. I. Tjelta, O. E. Hansteen und H. P. Jostad, „Observed platform response to a "monster" wave," in *Field Measurements in Geomechanics*, Lisse, Swets & Zeitlinger, 2003.

[4] B. W. Byrne und G. T. Houlsby, „Assessing Novel Foundation Options for Offshore Wind Turbines," Magdalen College, Oxford, 2006.

[5] R. B. Kelly, B. W. Byrne, G. T. Houlsby und C. M. Martin, „Tensile Loading of Model Caisson Foundation for Structures in Sand," Oxford University Department of Engineering Science, Oxford, 2004.

[6] G. T. Houlsby, R. B. Kelly und B. W. Byrne, „The Tensile Capacity of Suction Caissons in Sand under Rapid Loading," Oxford University Department of Engineering Science, Oxford, 2005b.

[7] G. T. Houlsby und B. W. Byrne, „Design Procedures for Installation of Suction Caissons in Sand," *Proceedings of the Institution of Civil Engineers*, 2005b.

[8] S. Henke, „Herstellungeinflüsse aus Pfahlrammung im Kaimauerbau," Technische Universität Hamburg-Harburg, Hamburg, 2009.

[9] P.-A. von Wolffersdorff, „A Hypoplastic Relation for Granular Materials With a Predefined Limit State Surface," *Mechanics of Cohesive-Frictional Materials*, pp. 251-271, 1969.

[10] A. Niemunis und I. Herle, „Hypoplastic Model for Cohesionsless Soils With Elastic Strain Range," *Mechanics of Cohesive-Frictional Materials*, pp. 279-299, 1997.

[11] T. Hamann und J. Grabe, „A simple dynamic approach for the numerical modelling of soil as a two-phase material," *Geotechnik, 36(3):180-191*, 2013.

[12] F. A. Villalobos, „Model testing of Foundations for Offshore Wind Turbines," University of Oxford, Oxford, 2006.

[13] American Petroleum Institute, „Recommended Practice for Planning, Designing and Constructing Fixed Offshore Platforms — Working Stress Design, Twenty-first Edition; Errata and Supplement 3," Beuth, Berlin, 2007.

[14] Det Norske Veritas, „Classification Notes No. 30.4 "Foundations"," Det Norske Veritas, Hovik, 1992.

[15] T. I. Tjelta, T. R. Guttormsen und J. Hemstad, „Large-Scale Penetration Test at a Deepwater Site," Houston, 1986.

